Direct Contrast Synthesis for Magnetic Resonance Fingerprinting

Patrick Virtue[1,2] , Jonathan I. Tamir[1], Mariya Doneva[3], Stella X. Yu[1,2] , and Michael Lustig[1]

[1]*Electrical Engineering and Computer Sciences, University of California, Berkeley;*

[2]*International Computer Science Institute, Berkeley;* [3]*Philips Research Europe, Hamburg*

Target Audience. Researchers and developers working to improve acquisition and reconstruction for fast and quantitative MRI.

Introduction. Magnetic resonance fingerprinting (MRF) can generate quantitative maps of tissue and system parameters (PD,T1,T2,B0,B1) from a single acquisition [1]. MRF also has the potential to replace standard radiological sequences by using the parameter maps to **indirectly synthesize** contrast images, such as T1- and T2-weighted images, Fig. 1, dotted-blue lines. The concept of MRI synthesis dates back to 1985 [2] and techniques such as QRAPMASTER [3] have recently been shown to produce clinically viable images [4]. MR fingerprinting data contains rich parametric information and can be used for contrast synthesis. However, MRI synthesis techniques from parameters are significantly limited by biases, due to effects that are difficult to simulate, such as time varying signals, partial voluming, flow, diffusion, magnetization transfer, and others. We propose training neural networks to **directly synthesize** contrast-weighted images from MRF data, bypassing insufficient parameter modeling, Fig. 1, solid-red line**.**

Methods. *Fingerprinting acquisition and training data.* We scanned 13 volunteers with a 1.5T Philips Ingenia scanner using 13 receive channels. We acquired four consecutive axial head sequences: T1-weighted spin echo, TE=15 ms, TR=450 ms; T2-weighted turbo spin echo, TE=110, TR=2212; fingerprinting balanced fast field echo (bFFE) sequence with 500 repetitions, constant TE=3.3 and TR=20, and smoothly varying flip angles between 0-60 degrees. The spiral MRF acquisition was reconstructed to image space after gridding and coil combination with Philips CLEAR. We used the data from 11 volunteers for training and validation and used the data from two volunteers only for the final test results.

Indirect Contrast Synthesis. We simulated MRF signals with the extended phase graph (EPG) algorithm [5][6], and used cosine similarity to match nearest neighbor as in [1]. The nearest neighbor maps were converted to T1-weighted and T2-weighted contrast images by simulating spin echo sequences: $PD\left(1 - e^{-\frac{TR-TE}{T1}}\right)e^{-\frac{TE}{T2}}$, where PD is the proton density.

Direct Contrast Synthesis. The neural network for direct contrast synthesis was trained on three million 3x3 patches from the *in vivo* MRF data using an architecture similar to the two-channel real/imaginary network from [7], Fig. 2.

Results. Direct contrast synthesis consistently produced higher quality results than the indirect contrast method, where T1-weighted and T2-weighted both contain significant artifacts, especially in the vasculature and cerebrospinal fluid (CSF), Fig. 3.

Discussion & Conclusion. We show that our deep learning model for direct contrast synthesis can bypass incomplete simulation models and their associated artifacts. We look forward to expanding our experiments to include additional training data as well as additional contrast images, such as FLAIR.

Figure 1. Contrast synthesis from MRF: indirect (blue-dotted lines) versus direct (solid-red line).

Figure 2. Neural network architecture for direct contrast synthesis. 3x3 spatial patches are flattened and passed through three convolutional layers and then three fully connected layers, resulting in a contrast value prediction for the center of the input patch. Between each layer is a ReLU non-linear filter. The number of feature channels are shown above each block, while the size of the temporal dimensions are shown below. An L2 loss function is used to penalize predicted values that do not match the acquired contrast value.
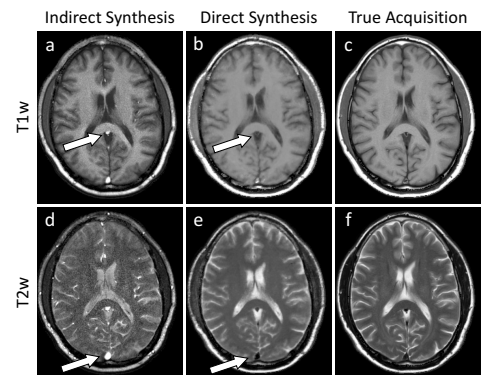
Figure 3. Results from indirect contrast synthesis (a,d) and direct contrast synthesis (b,e). Note that both indirect synthesis methods present inconsistent vessel contrast (white arrows), most noticeably in the superior sagittal sinus.

References. 1. D. Ma, V. Gulani, N. Seiberlich, K. Liu, J. L. Sunshine, J. L. Duerk, M. A. Griswold, "Magnetic Resonance Fingerprinting," Nature, vol. 495, no. 7440, pp. 187–192, 2013. **2.** S. A. Bobman, S. J. Riederer, J. N. Lee, S. A. Suddarth, H. Z. Wang, B. P. Drayer, J. R. MacFall, "Cerebral Magnetic Resonance Image Synthesis," AJN, vol. 6, no. 2, pp. 265–269, 1985. **3.** J. B. M. Warntjes, O. D. Leinhard, J. West, P. Lundberg, "Rapid Magnetic Resonance Quantification on the Brain: Optimization for Clinical Usage," MRM, vol. 60, no. 2, pp. 320–329, 2008. **4.** L. N. Tanenbaum, A. J. Tsiouris, A. N. Johnson, T. P. Naidich, M. C. DeLano, E. R. Melhem, P. Quarterman, S. X. Parameswaran, A. Shankaranarayanan, M. Goyen, A. S. Field, "Synthetic MRI for Clinical Neuroimaging: Results of the Magnetic Resonance Image Compilation (MAGiC) Prospective, Multicenter, Multireader Trial," AJN, 2017. **5.** J. Hennig, "Multiecho Imaging Sequences with Low Refocusing Flip Angles," JMR (1969), vol. 78, no. 3, pp. 397–407, 1988. **6.** M. Weigel, "Extended Phase Graphs: Dephasing, RF Pulses, and Echoes - Pure and Simple," JMRI, vol. 41, no. 2, pp. 266–295, 2015. **7.** P. Virtue, S. X. Yu, M. Lustig, "Better than Real: Complex-valued Neural Networks 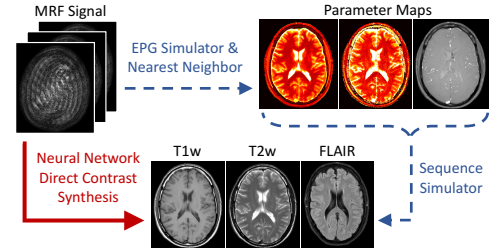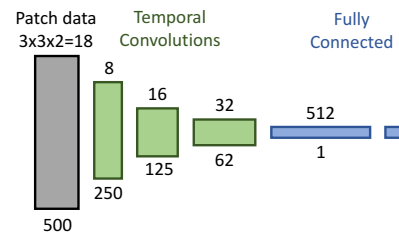for MRI Fingerprinting," ICIP, 2017